



A new upper limit for the rare decay $B_s^0 \rightarrow \mu^+ \mu^-$ using 2 fb^{-1} of Run II data

The DØ Collaboration
URL: <http://www-d0.fnal.gov>
(Dated: March 10, 2007)

We present in this note a new limit of the rare decay $B_s^0 \rightarrow \mu^+ \mu^-$ using about 2 fb^{-1} of Run II data collected with the DØ detector at the Tevatron. When setting limits on the branching ratio, selected events are normalized to reconstructed $B^\pm \rightarrow J/\psi K^\pm$ events resulting in a decreased systematic uncertainty. We obtain $\mathcal{B}(B_s^0 \rightarrow \mu^+ \mu^-) = 7.5 (9.3) \times 10^{-8}$ as a new upper limit at the 90% (95%) C.L.

Preliminary Results for Spring 2007 Conferences

I. INTRODUCTION

The purely leptonic decay $B_{d,s} \rightarrow \mu^+ \mu^-$ is a Flavor-Changing Neutral Current (FCNC) process [1]. In the Standard Model (SM), this decay is forbidden at the tree level and proceeds at a very low rate through higher-order diagrams. The SM branching ratio (\mathcal{B}) for this channel was first calculated in [2] and later refined to include QCD corrections [3]. The latest SM prediction [4] is, $\mathcal{B}(B_s \rightarrow \mu^+ \mu^-) = (3.42 \pm 0.54) \cdot 10^{-9}$, where the error is dominated by non-perturbative hadronic uncertainties. The corresponding leptonic branching fraction for the B_d meson is suppressed by an additional factor of $|V_{td}/V_{ts}|^2$ leading to an expected SM branching ratio of $(1.00 \pm 0.14) \cdot 10^{-10}$. Presently, the best published existing experimental bound for the branching fraction of B_s is $\mathcal{B}(B_s \rightarrow \mu^+ \mu^-) < 1.5 \cdot 10^{-7}$ at the 95% C.L. [5]. The best preliminary limit is from CDF and based on 780 pb^{-1} of integrated luminosity which allowed them to place an upper limit of $1.0 \cdot 10^{-7}$ at the 95% C.L. [6].

II. DETECTOR AND DATA SAMPLE

The DØ detector is described elsewhere [7]. The main elements, relevant for this analysis, are the central tracking and muon detector system. The central tracking system consists of a silicon microstrip tracker (SMT) and a central fiber tracker (CFT), both located within a 2 T superconducting solenoidal magnet. The muon detector located outside the calorimeter consists of a layer of tracking detectors and scintillation trigger counters in front of toroidal magnets (1.8 T), followed by two more similar layers after the toroids, allowing for efficient detection out to pseudorapidity (η) of about 2.0. In summer 2006 the SMT detector has been upgraded by inserting an additional layer of silicon strip detectors close to the beam pipe. Data taken before is referred to as Run IIa and the data taken afterwards is called Run IIb data. In Run IIb we also have tighter trigger requirements to deal with the increased instantaneous luminosity. The effective efficiency is therefore reduced in the Run IIb configuration due to the increased instantaneous luminosity, tighter trigger, and losses associated with commissioning of the new detector configuration. For Run IIb there also has been an upgrade in the trigger system at Level1 to cope with higher trigger rates.

The data in this analysis is the complete data sample up to the Jan. 6, 2007. The integrated luminosity of this sample is roughly 2 fb^{-1} .

For simulating the signal and normalization channels, Monte Carlo samples for the Run IIa and Run IIb configuration have been generated.

The two data samples are treated as two different and independent analyses, but the final limits are combined.

III. EVENT SELECTION

For the selection, we require the events to have fired a dimuon trigger. The pre-selection starts by requesting that the two identified muons match a central track and form a vertex. A cut is then applied to the mass spectra obtained by demanding the dimuon mass to be in the interval of 4.5 to 7.0 GeV/c^2 . The $\chi^2/d.o.f.$ of the two muon vertex is requested to be $\chi^2/d.o.f. < 10$. The transverse momentum of each of the muons is required to be greater than 2.5 GeV/c and their pseudorapidity has to be $|\eta| < 2.0$ to be well inside the fiducial tracking and muon regions. Tracks that are matched to each muon leg need at least three hits in the SMT and four hits in the CFT. For surviving events, the two-dimensional decay length L_{xy} in the plane transverse to the beamline is calculated. The error on the transverse decay length δL_{xy} is calculated by taking into account the uncertainties on both the primary and secondary vertex positions. The primary vertex itself is found with a beam spot constrained fit for each event, where the beam spot is obtained over the complete run. It is required that $\delta L_{xy} < 150 \mu\text{m}$. The transverse momentum of the B_s^0 candidate event needs to be greater than 5 GeV/c to ensure a similar p_T behavior of the $\mu^+ \mu^-$ -system in signal as well as in normalization channel events.

With these base requirements for the pre-selection we have in the Run IIa data set 163k candidate events and in the Run IIb data set 36k events.

To further reduce the background a likelihood discriminant is constructed using six variables. A likelihood ratio (LHR) is constructed as given by:

$$LHR = \frac{\prod_{i=1}^6 S_i(x)}{\prod_{i=1}^6 S_i(x) + \prod_{i=1}^6 B_i(x)} \quad (1)$$

where $S_i(x)$ (signal MC) and $B_i(x)$ (data mass sidebands) denote the i -th signal or background probability for an event. The probabilities are multiplied for each event and the ratio as given in Eq. 1 is calculated.

The variables used in the LHR are: *Isolation*, *Pointing angle*, *Transverse decay length significance*, *B impact parameter*, *minimal muon impact parameter* and a χ^2 *vertex probability* and are described in the following:

The isolation variable I of the muon pair is defined as:

$$I = \frac{|\vec{p}(\mu\mu)|}{|\vec{p}(\mu\mu)| + \sum_{\text{track } i \neq B} p_i(\Delta R < 1)},$$

The $\sum_{\text{track } i \neq B} p_i$, is the scalar sum of all tracks excluding the muon pair within a cone of $\Delta R < 1$ (where $\Delta R = \sqrt{(\Delta\Phi)^2 + (\Delta\eta)^2}$) around the momentum vector $\vec{p}(\mu^+\mu^-)$ of the dimuon pair. All tracks that are counted in the isolation sum have the additional requirement that the z distance of the track to the z -vertex of the muon pair has to be smaller than 5 cm in order to avoid tracks from additional ppbar interactions coming from the same bunch crossing.

The pointing angle α is defined as the angle between the momentum vector $\vec{p}(\mu^+\mu^-)$ of the dimuon pair and the vector \vec{l}_{Vtx} pointing from the primary vertex to the secondary vertex. If the muon pair is coming from the decay of a parent particle B_s , the vector \vec{l}_{Vtx} should point in the same direction as $\vec{p}(\mu^+\mu^-)$. The angle α is well-defined and used as a pointing consistency between the direction of the decay vertex and the flight direction of the B_s^0 candidate.

In order to discriminate against short-lived background, we used the transverse decay length significance $L_{xy}/\delta L_{xy}$ since it gives a better discriminating power than the transverse decay length alone. This length L_{xy} is defined as the projection of the decay length vector \vec{l}_{Vtx} on the transverse momentum of the B_s^0 -meson:

$$L_{xy} = \frac{\vec{l}_{Vtx} \cdot \vec{p}_T^{B_s^0}}{p_T^{B_s^0}}. \quad (2)$$

The error on L_{xy} , δL_{xy} is calculated by error propagation of the uncertainties on both the primary and secondary vertex position. The impact parameter of the B_s^0 candidate tends to be small; two random muons from background processes can have a larger impact parameter. If the muons are originating from a displaced secondary vertex, the impact parameter of these muons with respect to the primary vertex tends to be large. Therefore the minimal impact parameter significance to the two muons was used as an input variable to the LHR. The final variable for the LHR was a vertex probability that can be calculated for each secondary vertex using the $\chi^2/\text{d.o.f.}$ of the vertex fit.

The distribution for signal and background (data mass sideband) events of the LHR is given in Fig. 1. The distribution shows a peak at one where one expects signal and an other peak at zero, where the background is expected.

Between Run IIa and Run IIb, an additional inner layer of the SMT was installed providing the capability of additional measurement points at smaller radii. As expected, this improves the impact parameter resolution of the detector, reduces the uncertainty on the transverse decay length, and changes the probability distributions of some of the LHR variables as well as the performance of the LHR.

Two different optimization strategies using the LHR have been done. One optimization was performed on the ratio $\epsilon_{\mu\mu}/\langle n_{ul} \rangle$, where $\langle n_{ul} \rangle$ is the expected average upper limit given the expected background in the signal region. The second method was to maximize the criterion P proposed by G. Punzi [8]:

$$P = \frac{\epsilon_{\mu\mu}}{\frac{a}{2} + \sqrt{n_{back}}}. \quad (3)$$

Here, $\epsilon_{\mu\mu}$ is the reconstruction efficiency of the signal MC after the pre-selection and n_{Back} is the expected number of background events interpolated from the sidebands. The constant a is the number of sigmas corresponding to the confidence level at which the signal hypothesis is tested and was set to 2, corresponding to a 95% C.L.

1. Optimization

For the two different data sets two independent optimizations have been performed. The value of the selection cuts were the same in both optimizations. In Fig. 1 on the left side the LHR variable is shown for the Run IIa data set, and also indicating the best cut on $LHR > 0.946$, obtained from the optimization procedure. On the right side of Fig. 1 is the same distribution for the Run IIb data where the optimal cut value was found to be $LHR > 0.986$.

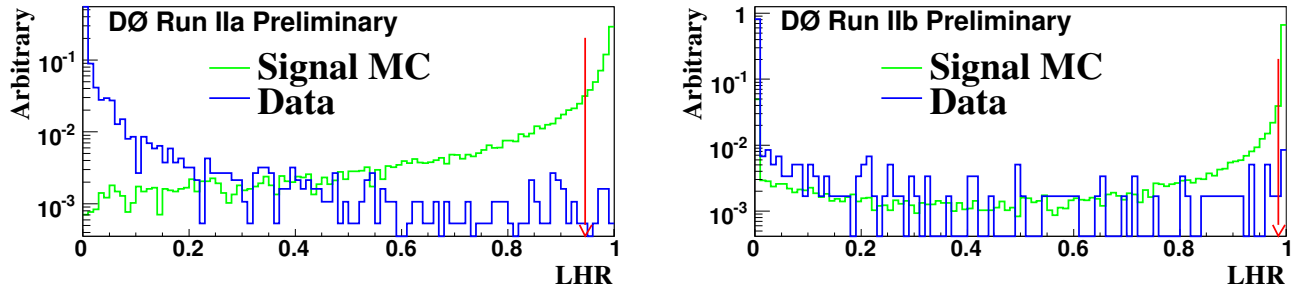


FIG. 1: The likelihood ratio distributions for signal MC and sideband data for Run IIa on the left side and Run IIb on the right side.

Region	min Mass (GeV/c^2)	max Mass (GeV/c^2)
blinded signal region for opti.	4.990	5.680
final signal region	5.047	5.622
sideband I	4.530	4.990
sideband II	5.680	6.370

TABLE I: The different dimuon invariant mass regions for signal and sidebands used for background estimation.

The expected background in the signal region was estimated using dimuon data from the sidebands of the mass histogram. Table I defines the regions for the sidebands and the signal regions that have been used.

After an exponential interpolation of the sideband population for the Run IIa data sample into the final signal region we obtain an expected number of background events of 0.8 ± 0.2 . The distribution of the remaining events is shown in Fig. 2 on the right side. Upon examination, one event was found in our search region, which is compatible with our background expectation of 0.8 ± 0.2 . On the left side of Fig. 2 the invariant mass as a function of the LHR is shown.

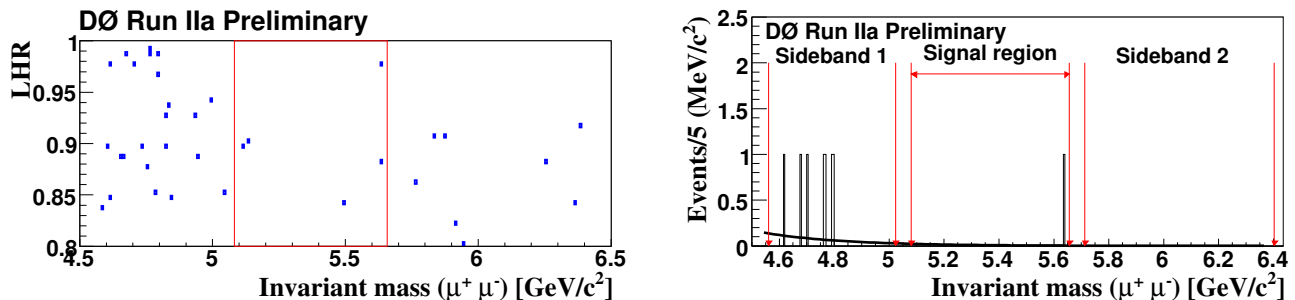


FIG. 2: The likelihood ratio as a function of the dimuon invariant mass on the left side and the di muon invariant mass spectrum of the surviving events on the right side for the Run IIa data set.

For the Run IIb data sample we found using a linear interpolation of the sideband population into the final signal region an expected number of background events of 1.5 ± 0.3 . A fit of an exponential function yields 1.1 ± 0.3 background events. The difference of these two fit models was taken as a systematic uncertainty. The distribution of the events (with the linear fit) is shown in Fig. 3. After we examined the signal region two events were found in our search region, compatible with our background expectation.

IV. THE NORMALIZATION CHANNEL $B^\pm \rightarrow J/\psi K^\pm$

To obtain a branching ratio limit for $B_s \rightarrow \mu^+ \mu^-$ we have used we have used the number of reconstructed $B^\pm \rightarrow J/\psi K^\pm$ events with $J/\psi \rightarrow \mu^+ \mu^-$ as normalization. The decay channel of $J/\psi \rightarrow \mu^+ \mu^-$ has the advantage that the efficiency to find and reconstruct the two muons cancels with the muons from the $B_s^0 \rightarrow \mu^+ \mu^-$ signal to a large extent. Therefore, we have applied the same cuts on the discriminating variables to the J/ψ 's from B^\pm 's as in the $B_s \rightarrow \mu^+ \mu^-$ search.

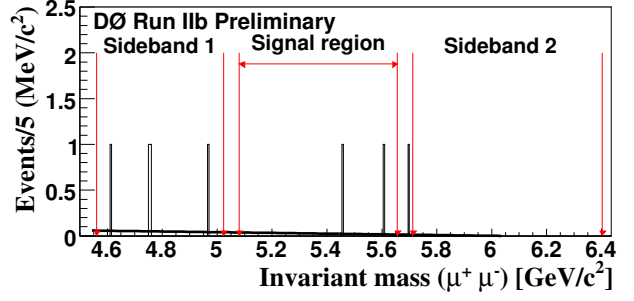
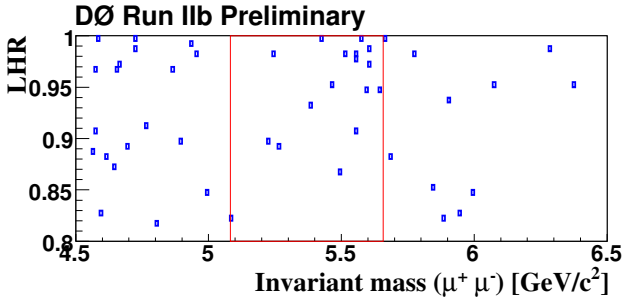


FIG. 3: The likelihood ratio as a function of the dimuon invariant mass on the left side and the di muon invariant mass spectrum of the surviving events on the right side for the Run IIa data set.

The J/ψ vertex fit of the two μ 's is requested to have a χ^2 of not more than 10 similar to the $\mu^+\mu^-$ vertex criterion in the B_s search. The combined vertex fit of the J/ψ and the additional K^\pm should not yield a χ^2 of more than 20. The p_T of the K^\pm should be larger than 0.9 GeV/c. Moreover, the collinearity angle between decay length vector of the B^\pm and the combined momentum of J/ψ and K^\pm in the transverse plane of greater than 0.9 is required.

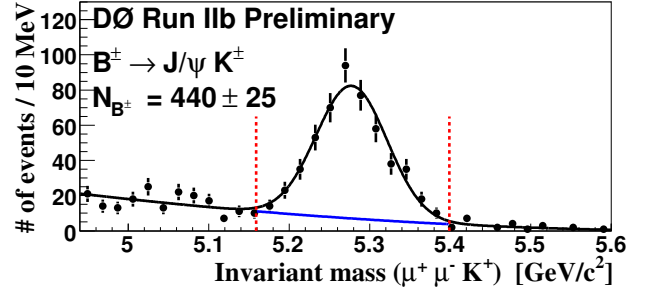
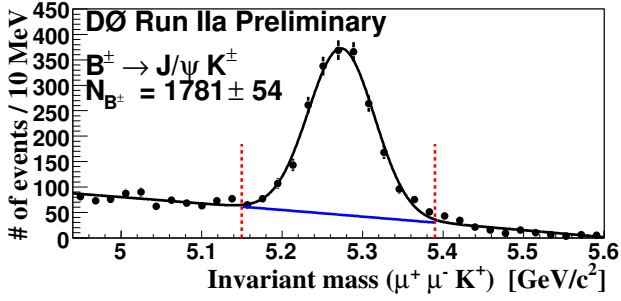


FIG. 4: The normalization channel $B^\pm \rightarrow J/\psi K^\pm$ for the Run IIa (left side) and Run IIb (right side) data sample.

The mass spectrum of the reconstructed $B^\pm \rightarrow J/\psi K^\pm$ for the Run IIa data sample is shown in Fig. 4 on the left side. A fit using a Gaussian function for the signal and a second order polynomial for the background yielded $1781 \pm 54 \pm 20$ B^\pm events, where the first uncertainty is statistical and the second due to systematics estimated by varying the fit range and background shape hypothesis. For the Run IIb data sample, the mass spectrum of the reconstructed $B^\pm \rightarrow J/\psi K^\pm$ is shown in Fig. 4 on the right side. A fit using a Gaussian function for the signal and a second order polynomial for the background yielded $440 \pm 25 \pm 5$ B^\pm events, the first uncertainty is again statistical and the second due to systematics.

V. CALCULATION OF THE LIMITS

A. The upper limit on the branching ratio

To calculate an upper limit on the $\mathcal{B}(B_s^0 \rightarrow \mu^+\mu^-)$ we normalize to the number of reconstructed events B^\pm decaying into $J/\psi(\mu^+\mu^-)K^\pm$ as explained in Section IV. Thus, $\mathcal{B}(B_s^0)$ can be calculated by:

$$\mathcal{B}(B_s^0) \cdot \left(1 + R \cdot \frac{\epsilon_{\mu\mu}^{B_d^0}}{\epsilon_{\mu\mu}^{B_s^0}} \cdot \frac{b \rightarrow B_d^0}{b \rightarrow B_s^0} \right) = \quad (4)$$

$$\frac{\mu(n_{signal}, n_{back})}{N_{B^\pm}} \cdot \frac{\epsilon_{\mu\mu K}}{\epsilon_{\mu\mu}^{B_s^0}} \cdot \frac{b \rightarrow B^\pm}{b \rightarrow B_s^0} \cdot \mathcal{B}(B^\pm \rightarrow J/\psi K^\pm) \cdot \mathcal{B}(J/\psi \rightarrow \mu\mu), \quad (5)$$

- $\epsilon_{\mu\mu}^{B_s^0}$ and $\epsilon_{\mu\mu K}$ are the efficiencies of the signal and normalization channels, obtained from MC simulations;
- $b \rightarrow B_s^0$, $b \rightarrow B^\pm$ and $b \rightarrow B_d^0$ are the fragmentation fractions of b or \bar{b} quark producing a B_s^0 , a B^\pm or a B_d^0 respectively. The ratio which enters in the equation has been calculated using the latest world average values [9]

for the fragmentation for $B_{u,d}$ and B_s^0 mesons respectively. We assume for the error on the fragmentation ratio a full anti-correlation between the two and obtain $f(b \rightarrow B_s^0)/f(b \rightarrow B_{u,d}) = 0.258 \pm 0.039$

- $\mathcal{B}(B^\pm \rightarrow J/\psi K^\pm) = (1.00 \pm 0.04) \cdot 10^{-3}$ and $\mathcal{B}(J/\psi \rightarrow \mu\mu) = (5.88 \pm 0.1)\%$ [9]; and
- $R \cdot \epsilon_{\mu\mu}^{B_d^0}/\epsilon_{\mu\mu}^{B_s^0}$ is the branching fraction ratio $\mathcal{B}(B_d^0)/\mathcal{B}(B_s^0)$ of $B_{d,s}^0$ mesons decaying into two muons [10] multiplied with their efficiency ratio.

To simplify the calculation of the upper limit on the branching fraction $\mathcal{B}(B_s^0 \rightarrow \mu^+\mu^-)$ in Eq. 4, it is assumed that there are no contributions from $B_d^0 \rightarrow \mu^+\mu^-$ decays ($R \approx 0$) in our search window centered around the B_s^0 mass. This assumption is acceptable since the decay is suppressed by $|V_{td}/V_{ts}|^2 \approx 0.04$. Any non-negligible contribution due to B_d^0 decays ($R > 0$) would make the obtained branching fraction $\mathcal{B}(B_s^0 \rightarrow \mu^+\mu^-)$ as given in Eq. 4 smaller. Thus, our presented limit for $\mathcal{B}(B_s^0 \rightarrow \mu^+\mu^-)$ can be considered conservative.

The efficiencies $\epsilon_{\mu\mu}^{B_s^0}$ and $\epsilon_{\mu\mu K}$ are the global signal efficiencies for the search signal and normalization channel respectively including the pre-selection cuts and the acceptance.

For the Run IIa dataset we obtain a total MC selection efficiency ratio of $\epsilon_{\mu\mu K}^{B^\pm}/\epsilon_{\mu\mu}^{B_s^0} = 0.173 \pm 0.005$ and for Run IIb we get $\epsilon_{\mu\mu K}^{B^\pm}/\epsilon_{\mu\mu}^{B_s^0} = 0.176 \pm 0.004$. To account for the tracking inefficiencies in our data sample, which are not present in our simulation, we estimated an efficiency for our third track from data. This was found by comparing the yield of J/ψ events with the yield of B^\pm events for Run IIa and Run IIb. It was found that our efficiency in Run IIb data to find the third track is 0.75 ± 0.10 with respect to Run IIa data. To take this effect into account, a scaling factor 0.75 ± 0.10 was applied to the efficiency ratio. For the data of Run IIb, we therefore obtained for the efficiency ratio $\epsilon_{\mu\mu K}^{B_s^0}/\epsilon_{\mu\mu}^{B_s^0} = 0.136 \pm 0.005$. The known Run IIb inefficiencies include those related to the tune-up of the new analogue front-end hardware that result from timing issues (unrecoverable for the data taken over the first two months of IIb operation) and CFT signal thresholds. The efficiency loss due to the latter effect is being recovered in an ongoing reprocessing of the Run 2b data collected up to Jan. 6, 2007. There are additional efficiency losses (e.g., high luminosity effects, trigger changes) and gains (additional track position measurements, new triggers, etc.), relative to the Run IIa data, that are estimated from data and the changes in the detector configuration.

B. Uncertainties and Limits

All the relative uncertainties that enter into the calculation of \mathcal{B} are given in Table II. Aside from the background uncertainty, the largest uncertainty common to the two data sets of 15% comes from the fragmentation ratio ($b \rightarrow B^\pm)/(b \rightarrow B_s^0)$. For the error on the fragmentation ratio we have assumed that the individual fragmentations ($b \rightarrow B^\pm$) and ($b \rightarrow B_s^0$) are anti-correlated with a correlation coefficient of $\rho = -0.5$ [11].

The relative statistical uncertainties on $\epsilon_{\mu\mu}^{B_s^0}$ and $\epsilon_{\mu\mu K}$ are 1.8% and 2.1% for Run IIa respectively and 1.2% and 1.5% for Run IIb. They are each combined into one efficiency uncertainty number assuming no correlations.

The value for the final efficiency ratio is then given for Run IIa by $\epsilon_{\mu\mu K}/\epsilon_{\mu\mu}^{B_s^0} = 0.173 \pm 0.005 \pm 0.009$, where the second error is due to systematics which arise from a different muon p_T distribution between J/ψ and B_s^0 decays (2.3%), the uncertainty on the tracking efficiency with respect to that predicted by the MC (1% for Run IIa), the weighting procedure (5.6%), and finally the uncertainty on trigger and muon identification between data and MC (0.7%).

For Run IIb we obtain $\epsilon_{\mu\mu K}/\epsilon_{\mu\mu}^{B_s^0} = 0.136 \pm 0.003 \pm 0.019$. The same systematic uncertainties as above have been taken into account. The uncertainty for the weighting procedure was estimated to be 4.8%. An additional uncertainty related to the scaling of our MC efficiency was added to the systematic uncertainty on the efficiency ratio. It was estimated to be 13.3% from the scaling factor and its uncertainty.

For Run IIa the relative uncertainty on the number of remaining background events is 25% and the B^\pm normalization channel has a relative uncertainty of 3.2% including statistical and systematical error. For Run IIb we find 33% for the background uncertainty, where the uncertainty of the fit (0.3 events) was combined with the uncertainty obtained with the different background description (0.4 events), and 5.7% for the normalization channel.

For the limit calculation we have propagated the theoretical errors on the fragmentation and branching ratios as well as the normalization error of the B^\pm into global signal and background efficiency uncertainties assumed to be of gaussian shapes. The modified probability function distributions are then obtained by integrating over those distributions. The limit calculation assumes a full correlation among the signal and background detection efficiencies. As previously mentioned we have used the program described in [12] for the calculation.

TABLE II: The relative uncertainties for calculating an upper limit of \mathcal{B} .

Source	Relative Uncertainty [%]	
	Run IIa	Run IIb
$\epsilon_{\mu\mu K}^{B^\pm}/\epsilon_{\mu\mu}^{B^0}$	6.7	5.9
Scaling of $\epsilon_{\mu\mu K}^{B^\pm}/\epsilon_{\mu\mu}^{B^0}$	–	13.3
# of $B^\pm \rightarrow J/\psi K^\pm$	3.2	5.7
$\mathcal{B}(B^\pm \rightarrow J/\psi K^\pm)$	4.0	4.0
$\mathcal{B}(J/\psi \rightarrow \mu\mu)$	1.7	1.7
$f_{b \rightarrow B_s^0}/f_{b \rightarrow B^\pm}$	15	15
background uncertainty	25	33

The statistical uncertainties on the background expectation as well as the uncertainties of signal and background efficiencies can be folded into the limit calculation of Eq. 4 by integrating over probability functions which parameterize the uncertainties. We have used a Bayesian approach [12] to perform the limit calculation and combination. The background is modeled as a Gaussian distribution with its mean value equal to the expected number of background events and its sigma equal to the background uncertainty. The signal and background efficiency uncertainties are considered as Gaussian distributions assuming a full correlation between the two. The uncertainty on the number of B^\pm events is propagated into the signal and background efficiency uncertainties. The relative errors on the fragmentation ratio and on the branching ratios are taken into account. Limits at 90% (95%) C.L. including statistical and systematic uncertainties are then set for the Run IIa data of

$$\mathcal{B}(B_s^0 \rightarrow \mu^+\mu^-)_{RunIIa} < 7.9 (9.5) \times 10^{-8},$$

and for the Run IIb data

$$\mathcal{B}(B_s^0 \rightarrow \mu^+\mu^-)_{RunIIb} < 3.1 (4.0) \times 10^{-7}.$$

Combining these two limits we obtain

$$\mathcal{B}(B_s^0 \rightarrow \mu^+\mu^-)_{2fb^{-1}} < 7.5 (9.3) \times 10^{-8}$$

We also quote the *single event sensitivity (ses)* of this analysis defined as the calculated value for $\mathcal{B}(B_s^0 \rightarrow \mu^+\mu^-)$ in Eq. 4 in the case of $\mu(n_{back}) = 1$. It is given by $ses = 2.2 \times 10^{-8}$ for Run IIa and $ses = 6.9 \times 10^{-8}$ for Run IIb and represents an inverse measure for the acceptance and efficiency factors of the analysis, but does not include any background conditions. The *ses* for Run IIa is approximately three times larger due to the larger integrated luminosity.

TABLE III: Summary information on the $B_s^0 \rightarrow \mu^+\mu^-$ analysis.

	Run IIa	Run IIb
$\frac{\epsilon_{\mu\mu K}^{B^\pm}}{\epsilon_{\mu\mu}^{B^0}}$	$0.173 \pm 0.005 \pm 0.009$	$0.136 \pm 0.003 \pm 0.019$
N_{B^\pm}	$1781 \pm 54 \pm 20$	$440 \pm 25 \pm 5$
N_{back}	0.8 ± 0.2	1.5 ± 0.5
N_{obs}	1	2
<i>ses</i>	2.2×10^{-8}	6.9×10^{-8}
limit 90% C.L.	7.9×10^{-8}	3.0×10^{-7}
limit 90% C.L.	7.5×10^{-8} (DØ comb.)	
limit 95% C.L.	9.5×10^{-8}	3.9×10^{-7}
limit 95% C.L.	9.3×10^{-8} (DØ comb.)	

VI. CONCLUSIONS

We have presented an update of the search for the rare decay $B_s^0 \rightarrow \mu^+\mu^-$. We have used a recorded dataset of approximately 2 fb^{-1} . For this data set the expected background interpolated from the sidebands amounts to 0.8 ± 0.2 events for Run IIa and 1.5 ± 0.5 events for Run IIb while we observe 1 and 2 candidates respectively. This is compatible with the background expectation; hence, we calculate the upper limit at a 90% (95%) C.L. of

$$\mathcal{B}(B_s^0 \rightarrow \mu^+\mu^-) < 7.5 (9.3) \times 10^{-8}. \quad (6)$$

This new upper limit improves the best published limits of $D\bar{O}$ by roughly a factor of 5.

The problem of reduced tracking efficiency of Run IIb data has been addressed and reprocessing will recover the tracking efficiency of the early fraction of Run IIb data. The final limit from Run IIb is expected to significantly improve per unit of luminosity than what is presented in this note.

We thank the staffs at Fermilab and collaborating institutions, and acknowledge support from the Department of Energy and National Science Foundation (USA), Commissariat à l'Énergie Atomique and CNRS/Institut National de Physique Nucléaire et de Physique des Particules (France), Ministry of Education and Science, Agency for Atomic Energy and RF President Grants Program (Russia), CAPES, CNPq, FAPERJ, FAPESP and FUNDUNESP (Brazil), Departments of Atomic Energy and Science and Technology (India), Colciencias (Colombia), CONACyT (Mexico), KRF (Korea), CONICET and UBACyT (Argentina), The Foundation for Fundamental Research on Matter (The Netherlands), PPARC (United Kingdom), Ministry of Education (Czech Republic), Natural Sciences and Engineering Research Council and WestGrid Project (Canada), BMBF and DFG (Germany), A.P. Sloan Foundation, Research Corporation, Texas Advanced Research Program, and the Alexander von Humboldt Foundation.

-
- [1] Charge conjugated states are included implicitly.
 - [2] B. A. Campbell and P. J. O'Donnell, Phys. Rev. D **25**, 1989 (1982).
 - [3] G. Buchalla and A. J. Buras, Nucl. Phys B **400**, 225 (1993); M. Misiak and J. Urban, Phys. Lett. B **451**, 161 (1999); G. Buchalla and A. J. Buras, Nucl. Phys. B **548**, 309 (1999).
 - [4] A. J. Buras, Phys. Lett. B **566**, 115 (2003).
 - [5] R. Bernhard *et al.*, arXiv:hep-ex/0508058.
 - [6] CDF public note 8176,
 - [7] V. M. Abazov *et al.* [D0 Collaboration], Nucl. Instrum. Meth. A **565** 463 (2006).
 - [8] G. Punzi, Talk given at the Conference on Statistical Problems in Particle Physics, Astrophysics and Cosmology (Phystat 2003), SLAC, Stanford, California, 8-11 September 2003, physics/0308063.
 - [9] W.-M. Yao *et al.*, Journal of Physics G **33**, 1 (2006).
 - [10] In the SM R is given by $R = \tau(B_d^0)/\tau(B_s^0) \cdot m_{B_d^0}/m_{B_s^0} \cdot F_{B_d^0}^2/F_{B_s^0}^2 \cdot |V_{td}|^2/|V_{ts}|^2$, where $\tau_{B_{d,s}^0}$ are the lifetime of the B -mesons and $F_{B_{d,s}^0}$ are the meson decay constants. The relation on the branching fraction ratio holds in fact for all new physics that is obeying MFV [4].
 - [11] Heavy Flavour Averaging Group, http://www.slac.stanford.edu/xorg/hfag/osc/PDG_2006/index.html#FRAC
 - [12] T. Hebbeker, L3 Note 2633, (2001).